

A study of mesoscale gravity waves over North Atlantic with satellite observations and a mesoscale model

Dong L. Wu¹ and Fuqing Zhang²

¹ Jet Propulsion Laboratory, California Institute of Technology, Pasadena, CA

² Department of Atmospheric Sciences, Texas A&M University, College Station, TX

June 4, 2004

Submitted to *Journal of Geophysical Research*

Key words: mesoscale gravity waves, satellite observations, North Atlantic

1. Introduction

Gravity waves (GWs) play important roles in determining atmospheric circulations and thermal structures. Since many of these waves are not resolved in global climate and weather prediction models, the momentum and energy releases from the wave breaking must be incorporated through subgrid-scale parameterizations (e.g., Hamilton, 1996; McLandress, 1998; Kim et al., 2003). In addition, GW processes have direct impacts on mesoscale precipitation bands and can be coupled with severe convection in the troposphere (Bosart et al., 1998). Their role on formation of polar stratospheric clouds, which are important to ozone chemistry (Leutbecher and Volkert, 2000; Dörnbrack *et al.*, 2002), remain to be quantified.

GW excitations are mostly related to processes of convection, jetstream, and flow over orography in the lower atmosphere (Fritts and Alexander, 2003; and references therein). However, knowledge of global distributions and properties of these wave sources remains poor, which is a major uncertainty for accurate GW drag parameterizations. Current GW parameterization schemes are simplified, semi-arbitrary, and lacking observational guidance. More quantitative studies are needed for a comprehensive understanding of these wave processes between their genesis in the troposphere and propagation/breaking in the upper stratosphere. It is required, therefore, for these observational and modeling investigations to cover a broad vertical and horizontal domain from the surface to the mesosphere with sufficient resolutions.

Mesoscale models (e.g., PSU/UCAR mesoscale model MM5) on a domain as large as a hemisphere can simulate realistic GWs in the troposphere and stratosphere, and have been the primary tool for studying wave generation and propagation mechanisms (e.g.,

Zhang and Fritsch, 1988; Schmidt and Cotton, 1990; Zhang 2004). Mesoscale models can reveal detailed wave structures, energy sources, and maintenance mechanisms that are difficult to measure by satellite sensors (Zhang and Koch, 2000; Koch et al, 2001; Zhang et al. 2001; Zhang et al. 2003). Some specialized wave models (e.g., Mountain-wave Forecast Model) have also been used to study wave propagation properties from the source region to as high as the thermosphere (Eckermann and Pressue, 1999).

Modeled GW properties and effects require observational verifications that are rarely available. Assimilated or analysis/reanalysis datasets often have biases from the models. Mesoscale phenomena in these datasets depend largely on the rejection criteria used. Conventional observations (e.g., radiosondes) provide little reports over oceans and integrated GW forcing. Because of limited height coverage of the ground-based measurements, the faith of large-amplitude GW events and their impacts on dynamics in the stratosphere and mesosphere were little explored. In addition, substantial uncertainties exist in the commonly-used hodograph method to retrieve GW characteristics from the sounding profiles (e.g., Zhang et al. 2004).

Satellite observations provide a valuable source for GW studies in the middle and upper atmosphere, especially over oceans and other radiosonde-sparse regions. Recent space techniques offer appreciable resolution and precision for observing mesoscale GWs on a global basis. Among satellite sensors, passive microwave sounders have been successfully utilized to observe GW activity in the stratosphere, e.g., Microwave Limb Sounder (MLS) (Wu and Waters, 1996; McLandress et al., 2000; Jiang et al., 2004) and Advanced Microwave Sounding Unit-A (AMSU-A) down to the tropopause (Wu, 2004). These studies analyzed raw radiance measurements, rather than retrieved temperature, to

infer air temperature perturbations, where most GW information is preserved. Because mesoscale features are often transient and weak in amplitude, it is important in satellite data analyses not to introduce additional error (e.g., retrieving atmospheric temperature). These extra data manipulations would smear out mesoscale signatures of interest and make the results complicated to interpret.

In this paper we present an observational study of mesoscale gravity waves over North Atlantic (NA) using radiances measured by MLS and AMSU-A for the period of December-January (section 2). The study is focused on an event on 19-21 January 2003 when an upper-level trough swept through East Coast of the United States (section 3). Large-amplitude GWs excited in this period have multiple components, which are associated strongly with jet streak, orographic forcing, and convective activity in the troposphere. Preliminary simulations from MM5 are made for the 19-21 January 2003 event and compared to the AMSU-A observations. Wave generation mechanisms and the roles of a strong upper-tropospheric jet streak are discussed in section 5.

2. MLS and AMSU-A GW observations of December 2002 and January 2003

The 63-GHz O₂ radiances measured by MLS on the Upper Atmosphere Research Satellite (UARS) are sensitive to temperature perturbations induced by waves of short (< 100 km) horizontal and long (> 10 km) vertical wavelengths (Wu and Waters, 1996). These radiance perturbations have been used to produce GW variance maps in the stratosphere and mesosphere (McLandress et al., 2000; Jiang et al., 2004). Much of the MLS GW variances in the Northern Hemisphere (NH) winter were thought of orographic origin (Jiang et al., 2004), and overall good agreement was found over elevated terrains in comparison with the Naval Research Laboratory Mountain Wave Forecast Model

(MWFM). For example, during December 1991-January 1992, the MLS GW variance maps show clear enhancements over mountains in Alaska, Canada, Greenland, Scandinavia and Russia [Figure 1].

However, GWs over oceans (e.g., the NA region) have not been investigated in detail and the link of these waves between in the troposphere and in the stratosphere is not clear. In the stratosphere, the NA wave activity is clearly evident in Figure 1, where enhanced GW variance extended from Canada to south of Greenland. This feature appeared in every winter season during 1991-1994. The NA component becomes increasingly important as waves propagate to higher altitudes. At 61 km the NA component and the east coast of United States make up ~20% of the total wave variance at latitudes of 30°N-70°N.

To explore GW activity at lower altitudes, Wu [2004] applied the MLS analysis method to AMSU-A radiance data that have better horizontal resolution and longer records. The AMSU data are particularly useful for studying mesoscale GWs of long (>10 km) vertical wavelengths. Its global coverage is excellent with almost no gaps between orbits and AMSU-A has 6 sounding channels covering altitudes of 18-45 km. GWs are generally detectable if amplitudes greater than the instrument noise (varying between 0.15 K for channel 9 and 0.8 K for channel 14). However, it requires some caution to analyze AMSU-A channels 1-8 since cloud and surface emission may affect the radiances considerably. Despite the improved coverage, the AMSU-A measurements still under-sample temporally most of mesoscale GWs (periods of 1-6 h and phase speeds of 10-40 m/s). Therefore, three-dimensional (3-D) snapshots of wave structures are very

valuable information for understanding and quantifying these wave generations and properties.

Shown in Figure 2 are AMSU-A GW variance maps at 80 hPa (~18 km) and 5 hPa (37 km) during December 2002-January 2003. These AMSU-A variances are obtained from radiance fluctuations sampled at 32°-48° viewing angles (with respect to nadir), instead the limb case (~66° from nadir) as for MLS. The viewing angle is important in terms of radiance sensitivity to GW-induced temperature perturbations because the radiance perturbations are resulted from convolution between 3-D wave structures and instrument weighting functions.

The 37-km AMSU-A map exhibits the climatology similar to MLS observations in the 1991-1992 winter, showing the stronger NA contribution than MLS. In the 18-km map, orographic sources clearly stand out as enhanced activities near elevated terrains, including the southern Andes, New Zealand, the Appalachians, the southern Greenland, Scandinavia, Urals, Putoran, Zagros, Himalayas, and Japan. Most of these mountain waves did not propagate above 37 km, except maybe over Scandinavia, Urals and Putoran. The enhanced GWs at 37 km are consistent with the MLS observations. In addition to orographic components, there are weak but significant enhancements in the Southern Hemisphere (SH) subtropics from deep convection, which appear both in the MLS maps and in the AMSU-A maps. These convectively generated GWs have been investigated previously with MLS data (McLandress et al., 2000; Jiang et al., 2004).

Despite differences in viewing geometry and observing period, the MLS and AMSU-A maps reveal strikingly similar GW distributions in the NH stratosphere, both showing significant wave activity over NA in the December-January months. These results raise

important questions about causes of these waves in the troposphere and their impacts on upper atmospheric dynamics. What are the excitation mechanisms of these mesoscale GWs, how frequent are these excitations, and how much reach or break in the stratosphere and above? Motivated by these questions, we conduct a detailed investigation utilizing AMSU-A observations and MM5 simulations on the large-amplitude GW event on 19-21 January 2003.

3. The 19-21 January 2003 Event

In the troposphere, large-amplitude wave events are infrequent but may be persistent and maintained for a relatively long (1-3 days) period of time (Ramamurthy et al. 1993; Koppel et al. 2000). These waves typically have wavelengths of 50–500 km, periods of 0.5–4 h, surface amplitudes of 0.5–15 hPa, and phase velocities of 15–35m/s, and are capable of organizing precipitation into bands, creating damaging winds, sleet and blizzard conditions, and triggering instabilities that lead to the development of severe convection in the downstream. The situation becomes more complex when sensible heating over elevated terrain is involved. According to the survey compiled by Uccellini and Koch (1987), these large-amplitude waves tend to appear in the vicinity of jet streaks and within the cool side of a surface warm or stationary front.

3.1 Meteorological conditions

During 18-20 January 2003, a long-wave, fast traveling upper trough moved into the eastern United States [Figure 3]. A strong jet with speed > 70 m/s was developed at 300 hPa, setting up favorable conditions for the jet-streak GW genesis in the upper troposphere. The left exit region of the jet is interesting to watch in launching upper jet waves. This synoptic scale feature affected a large area of North America and heavy

snowfalls in the East Coast were reported. Moving eastward, the trough on 20 January 2003 caused strong winds right toward Appalachians, setting up a perfect condition for launching mountain waves.

A similar strong cyclone-related GW event on 4 January 1994 was documented by Bosart et al. (1998), when heavy snowfall was reported along the Appalachians on the west side of wave fronts. The phase speed of these GWs was reported around 35-40 m/s with complex mesoscale structures imbedded in the cyclone environment. Using mesoscale model simulations with MM5, Zhang et al. (2001) proposed a complex sequence of geostrophic adjustment processes associated with the upper tropospheric jet streak are responsible for initiating the gravity waves.

3.2 AMSU-A Radiance Perturbation Maps

Four similar AMSU-A instruments are currently in operation: three on NOAA N15 (since May 1998), N16 (since September 2000) and N17 (since June 2002) satellites, and one on NASA Aqua satellite (since May 2002), with the ascending equator-crossing time at 1930, 1400, 2200, and 1330, respectively. As a result, the NA region is sampled every ~4 hours jointly by these instruments. The NOAA AMSU-A scan swath of ~2,300 km cross track, and each FOV produces a footprint size of ~50 km at nadir and ~110 km for the outermost beam with a scan angle of 48.3° from nadir.

To extract GW features from the AMSU-A radiances, the background radiance needs first to be determined. It is important not to use radiative transfer models for obtaining such background because the real atmosphere is unknown and the models could misrepresent the situation. Instead, we choose an empirical method for the background calculation, which uses a 2-D running mean on the raw radiance data. For this study, a 9-

point running window is used, which smoothes out most wave scales $< \sim 600$ km. Hence, the difference between the measured and smoothed radiances (i.e., the radiance perturbation) contains most fluctuations at scales $< \sim 600$ km. Since AMSU-A has a finite (30) number of cross-track measurements, the 2-D smoothing method needs to be replaced by the 1-D smoothing (along track) at the edges of the swath (4 FOVs on each side). The same 9-point truncation length is used for the 1-D smoothing. Such the smoothing method will remove the systematic effect, the so-called “limb” and “cross-track-asymmetry” effects (Goldberg et al., 2001).

Figure 4 shows four radiance perturbation maps of AMSU-A channel 9 (~ 80 hPa) during 19-20 January 2003. Two wave events are observed at this level during the period of interest. The first started on 19 January along the offshore of the East Coast with wave fronts lined up in the southeast-northwest direction. It propagates away from the continent at a phase speed of ~ 15 m/s, which can be estimated from consecutive orbits (~ 1.5 h difference) of the same satellite or adjacent orbits from different satellites. The second event occurred on 20 January near the Appalachians with wave fronts along the mountain ridge. These waves were further enhanced on late 20 and early 21 January 2003 over North Carolina and Georgia of the U.S. Other wave activities are also evident in this period, for example, near the Rockies and in Canada, but they exhibit somewhat weaker amplitudes.

Aloft, AMSU-A channel 13 (~ 5 hPa) radiances show amplified but delayed perturbations [Figure 5] after the wave appeared at 80 hPa. Wave characteristics have changed somewhat at this altitude, compared to the events seen by channel 9. Waves from the first event exhibit similar wavelength, phase speed and propagation direction,

but last slightly longer. It reaches the southern tip of Greenland before its breakdown in that neighborhood. Waves associated with the Appalachians propagate only a little away from their source region, and exhibit a different (south-north) alignment in wave fronts compared to those observed by channel 9. This perturbation begins to show a wake-like structure at ~17Z on 20 January, suggesting that this source is localized in a narrow region.

3.3 Wave structures and propagation

Figure 6 shows a close view of a snapshot of the NA wave at 6.5Z on 20 January 2003 from 6 pressure levels. The estimated horizontal wavelength ranges between 300 and 600 km. The event is dominated by a 500-km component, co-existing with other wavelengths. At 5 hPa waves of large amplitudes spread to a wider area than those at 80 hPa but location of the maximum amplitudes at 5 hPa seems to correspond well to the maxima at 80 hPa in general.

Figure 7 is the vertical cross-section of wave amplitudes from radiance perturbations in channels 7-14, showing upstream-tilted phase lines. These waves appear to have long (20-30 km) vertical wavelengths λ_z , which represent a very different class of mesoscale GWs from those $\lambda_z=2-5$ km waves studied elsewhere (e.g., Uccellini and Koch, 1987) in the low and middle troposphere. These long- λ_z GWs are ideal for instruments like AMSU-A to measure since its temperature weighting functions have thickness > 10 km.

We use all the AMSU-A observations on NOAA-15, 16, 17, and NASA Aqua satellites to monitor propagation of the primary wave component at 5 hPa. The wave track is shown in Figure 8. We start tracking this wave event at 5.6Z on 20 January after it was initiated near Newfoundland around 16Z on 19 January. This wave event lasted for

nearly two days and was maintained at a coherent phase speed between 5 hPa and 80 hPa during traveling. During the fast traveling period (11Z -16Z on 20 January), it posted a group velocity of ~ 40 m/s, which is somewhat greater than the phase speed estimated above from channel 9 observations.

3.4 Time series

In addition to wave generation, wave impacts on the upper air dynamics are important as well. We identify two regions, highlighted in Figures 4-5, to monitor wave amplitude variations over time. It clearly is shown in Figure 9 that the 19-21 January event was the exclusive disturbance over the entire East Coast and the NA region in terms of amplitude and duration. Tropospheric forcings are directly responsible for the large GW variances seen in the stratosphere in the same region [Figure 10]. However, the stratospheric responses were somewhat selective as stratospheric waves depend not only on wave source but also on the background winds that affect their propagation and breaking properties.

Unlike the broad and persistent enhancements at 80 hPa, the 5-hPa variances show sharp peaks with a shorter duration in region 1 and three transient peaks in region 2, each separated by ~ 18 h. The peak in region 1 and the first spike in region 2 are related, corresponding to waves propagating off the east coast with the fast horizontal speed described in Figures 6-8. The first event in region 2 leads in time the peak in region 1 peak as expected for the waves propagating from region 2 to region 1. The second and third spikes in region 2 are likely of orographic origin with small horizontal speeds since they did not propagate far enough to reach region 1. They remain in the same region, and

the enhanced channel 9 and 13 variances exhibit little time delay, suggesting the fast stratospheric response to disturbances from the troposphere.

3.5 MM5 simulations

The NCAR/PSU nonhydrostatic model MM5 version 3 (Dudhia 1993) is used to investigate the large-amplitude GW event that occurred on 19-21 January 2003 in the East Coast of the United States and over NA. MM5 has been demonstrated for its capability of simulating realistic wave phenomena associated with baroclinic jet-front systems in previous studies (e.g., Zhang et al. 2001). For this study, the MM5 model domain employs 300×200 grid points with 30-km horizontal grid spacing and 90 vertical layers equally spaced from the surface up to 10 hPa, covering the entire North America, NA and adjacent regions. The ECMWF analysis (archived at NCAR on a 2.5 degree by 2.5 degree grid) is used to provide the initial and boundary conditions for the simulations. The MM5 is initialized at 0Z 19 January 2003 and integrated for 36 h. The MRF PBL scheme (Hong and Pan 1996), Grell cumulus parameterization scheme (Grell 1993), and Reisner microphysics scheme (Reisner et al. 1998) are used in this event simulation.

The MM5 simulation is verified well at large scales against the ECMWF analysis throughout the 36-h model integration (not shown). In particular, they both simulated well the strength and location of the upper-tropospheric jet streak. Inertia-GWs are found in the MM5 simulation in the divergence maps (e.g., alternating bands of convergence and divergence), as well as in wind and temperature fluctuations throughout the troposphere and stratosphere. Figure 11 shows the MM5 simulated 80-hPa horizontal divergence overlaid with upper-tropospheric (300 hPa) jet streak valid at 18Z 19 January 2003. GW activities are pronounced in several regions, including the Rockies on the far

right edge of the Polar jet, the Appalachians right ahead of the Polar jet and behind the subtropical jet, and North Atlantic slightly to the left exit regions of the main subtropical jet. These GWs are in qualitative agreement with the AMSU-A observations despite a slight eastward shift in location for the NA wave packets.

This flow configuration over the NA and near the East Coast of the U. S. is conducive to GW generation, as shown by Uccellini and Koch (1987) and Zhang (2004). As indicated in the AMSU-A observations, these GWs are propagating east and northeastward relative to the ground. The maximum amplitudes of the wind and temperature perturbations found in the simulation are 10 ms^{-1} and 5 K, respectively. The horizontal wavelengths of these waves are approximately 300-400 km. Figure 12a displays a vertical cross section at the same time through the center of the wave packets and along the direction of wave propagation just offshore of the Atlantic Coast of the U. S. The vertical wavelength shown in Figure 12a is approximately 8-10 km, which is also in agreement with the AMSU-A observations.

In the MM5 simulation, mountain waves over the Appalachians exhibit the dominant horizontal wavelength of ~ 250 km and vertical wavelengths of > 10 km [Figure 12b]. These waves are transient, as shown in the satellite data, and localized within 1-2 wavelengths from the mountain source. The waves are mostly amplified on the lee side and tilted towards upstream. Unfortunately, the vertical extent of the current MM5 simulation is not high enough to determine the fate of these mountain waves and to assess their impacts on the upper air dynamics.

4. Summary and Discussion

Climatology and variability of the middle-atmospheric GWs over North America and the Atlantic Ocean are analyzed with MLS and AMSU-A radiance measurements during the December-January period. The satellite observations reveal detailed information on wave structures at 80-2 hPa in the 19-21 January 2003 event, showing horizontal wavelengths of 300-600 km and vertical wavelengths of 20-30 km. Besides the geographical modulation above regions of significant topography, these middle-atmospheric GWs are strongly correlated with intensity and location of the tropospheric baroclinic jet-fronts systems. The large-amplitude gravity wave event on 19-21 January 2003 over NA and the east coast of the United States is a good example of this kind. AMSU-A data show that these wave events, normally lasting for 1-2 days, can reach the upper stratosphere and cause unusual mesoscale disturbances at high altitudes.

A state-of-the-art mesoscale model is used to explicitly simulate this episode of enhanced GW activities identified from satellite observations. The simulated GWs compared qualitatively well with the satellite observations in terms of wave structures, timing, and overall morphology. Excitation of these large-amplitude mesoscale waves is complicated, and multiple mechanisms have been offered to explain their occurrences. The primary mechanisms include geostrophic adjustment (e.g., Zhang et al. 2001; Zhang 2004), shearing instability (e.g., Einaudi et al. 1987), frontogenesis and frontal collapse (e.g., Snyder et al. 1993), and convection (e.g., Powers and Reed 1993). Preliminary MM5 results suggest four likely source mechanisms for the 19-21 January 2003 GW event: (1) topographically-forced waves due to jet streaks incepted by large terrains; (2) adjustment-forced waves due to strong flow imbalance associated with the upper-tropospheric jet streaks; (3) diabatically-forced GWs due to moist convection induced by

baroclinic waves; and (4) frontally-forced GWs due to frontal collapse near the surface. The last three mechanisms are transient in nature and often inseparable from each other. These potential wave generation mechanisms are currently being investigated with explicit high-resolution mesoscale simulations and advanced diagnostics, which will be reported elsewhere. Moreover, impacts of these large-amplitude waves on the upper atmospheric dynamics and their interactions with larger-scale waves also warrant further investigations.

Acknowledgments

This work was performed partly at the Jet Propulsion Laboratory, California Institute of Technology, under contract with the National Aeronautics and Space Administration (NASA). We would like to acknowledge the supports from NASA ACPMAP program (DLW) and NSF Grant ATM-0203238 (FZ). We also thank NOAA Satellite Active Archive center for making the AMSU data available to this research.

References

- Bosart L. F., W. E. Bracken, and A Seimon, A study of cyclone mesoscale structure with emphasis on a large-amplitude inertia-gravity wave *Mon. Wea. Rev.*, **126**, 1497-1527, 1999.
- Dörnbrack, A., Birner, T., Fix, A., Flentje, H., Meister, A., et al., Evidence for Inertia Gravity Waves Forming Polar Stratospheric Clouds over Scandinavia. *J. Geophys. Res.*, **107**, D20 (10.1029/2001JD000452), 2002.
- Dudhia, J., A nonhydrostatic version of the Penn State/NCAR mesoscale model: Validation tests and simulation of an Atlantic cyclone and cold front. *Mon. Wea. Rev.*, **121**, 1493-1513, 1993.
- Eckermann, S. D., and P. Preusse, Global measurements of stratospheric mountain waves from space, *Science*, **286**, 1534-1537, 1999.
- Einaudi, F., W. L. Clark, D. Fua, J. L. Green, and T. E. VanZandt, Gravity waves and convection in Colorado during July 1983. *J. Atmos. Sci.*, **44**, 1534-1553, 1987.
- Fritts, D. C., and M. J. Alexander, Gravity wave dynamics and effects in the middle atmosphere. *Rev. Geophys.* **41** (1), 1003, doi:10.1029/2001RG000106, 2003.
- Goldberg, M. D., D. S. Crosby, and L. Zhou, The Limb Adjustment of AMSU-A Observations: Methodology and Validation. *J. Appl. Meteor.*, **40**, 70-83, 2001.
- Grell, G.A, Prognostic evaluation of assumptions used by cumulus parameterizations. *Mon. Wea. Rev.*, **119**, 5-31., 1993.
- Hong, S.-Y., and H.-L. Pan, Nocturnal boundary layer vertical diffusion in a medium-range forecast model. *Mon. Wea. Rev.*, **124**, 2322-2339, 1996.
- Jiang, J.H, S.D. Eckermann, D.L. Wu, and J. Ma, "A Search for Mountain Waves in MLS Stratospheric Limb Radiances from the Winter Northern Hemisphere: Data Analysis and Global Mountain Wave Modeling," *J. Geophys. Res.* **109**, D3, D03107, 10.1029/2003JD003974, 2004.
- Kim, Y.-J., S. D. Eckermann, and H.-Y. Chun, An overview of the past, present and future of gravity-wave drag parameterization for numerical climate and weather prediction models, *Atmos. Ocean*, **41**, 65-98, 2003.

- Koch S. E., F. Zhang, M. L. Kaplan, Y.-L. Lin, R. Weglarz, and C. M. Trexler,
 Numerical simulation of a gravity wave event observed during CCOPE. Part 3:
 Mountain-plain solenoids in the generation of the second wave episode. *Mon.
 Wea. Rev.*, **129**, 909–932, 2001.
- Koppel L. L., L. Bosart, and D. Keyser, A 25-yr Climatology of large-amplitude hourly
 surface pressure changes over the conterminous United States. *Mon. Wea. Rev.*,
96, 51–68, 2000.
- Leutbecher, M., and H. Volkert, The propagation of mountain waves into the
 stratosphere: quantitative evaluation of three-dimensional simulations, *J. Atmos.
 Sci.*, **57**, 3090-3108, 2000.
- McLandress, C., M. J. Alexander, and D. L. Wu, Microwave limb sounder observations
 of gravity waves in the stratosphere: a climatology and interpretation, *J. Geophys.
 Res.*, **105**, 11947-11967, 2000.
- Powers J. G., and R. J. Reed, Numerical model simulation of the large-amplitude
 mesoscale gravity-wave event of 15 December 1987 in the central United States.
Mon. Wea. Rev., **121**, 2285–2308, 2001
- Ramamurthy, M. K., R. M. Rauber, B. P. Collins, and N. K. Malhotra, A comparative
 study of large-amplitude gravity-wave events. *Mon. Wea. Rev.*, **121**, 2951–2974,
 2001.
- Reisener J, Rasmussen RJ, and Brintjes RT, Explicit forecasting of supercooled liquid
 water in winter storms using the MM5 mesoscale model. *Quart. J. Roy. Meteor. Soc.*,
124B, 1071-1107, 1998.
- Snyder, C., W. C. Skamarock, and R. Rotunno, Frontal dynamics near and following
 frontal collapse. *J. Atmos. Sci.*, **50**, 3194-3212, 1993.
- Uccellini L. W., and S. E. Koch, The synoptic setting and possible source mechanisms
 for mesoscale gravity wave events. *Mon. Wea. Rev.* **115**, 721–729, 1987.
- Wu, D. L., and J. W. Waters, Satellite observations of atmospheric variances: A possible
 indication of gravity waves, *Geophys. Res. Lett.*, **23**, 3631-3634, 1996.
- Wu, D. L., Mesoscale Gravity Wave Variances from AMSU-A Radiances. *Geophys. Res.
 Lett.*, in press, 2004.

- Zhang, F., Generation of mesoscale gravity waves in the upper-tropospheric jet-front systems. *J. Atmos. Sci.*, **61**, 440-457, 2004.
- Zhang F., and S. E. Koch, Numerical simulations of a gravity wave event over CCOPE. Part II: Waves generated by an orographic density current. *Mon. Wea. Rev.* **128**, 2777–2796, 2000.
- Zhang, F., S. E. Koch, and M. L. Kaplan, Numerical simulations of a large-amplitude gravity wave event. *Meteor. Atmos. Phys.*, **84**, 199-216, 2003.
- Zhang, F., S. Wang, and R. Plougonven: Uncertainties in using the hodograph method to retrieve gravity wave characteristics from individual soundings. *Geophys. Res. Lett.*, in press, 2004.
- Zhang F, S. E. Koch, C. A. Davis and M. L. Kaplan, Wavelet analysis and the governing dynamics of a large amplitude mesoscale gravity wave event along the East Coast of the United States. *Quart. J. Roy. Met. Soc.*, **127**, 2209–2245, 2001.

Figure Captions

Figure 1 GW variance maps from UARS MLS descending orbits for December 1991-January 1992 at 38 km (a), 48 km (b) and 61 km (c). The region over the northwestern Atlantic, highlighted by the circle, is of interest in this study where GWs are frequently generated and propagate into the stratosphere and mesosphere.

Figure 2 AMSU GW variance maps for December 2002-January 2003 at 80 hPa (~18 km) (a) and 5 hPa (~37 km) (b). Bad measurements are indicated by the white boxes.

Figure 3 ECWMF 300-hPa geopotential heights (every 20 dam) and horizontal winds (in vectors, speed greater than 60 m/s shaded) at (a) 0Z on 19 January and (b) 12Z on 20 January 2003. At 12Z on 20 January 2003, the trough moved to the east U.S, creating strong winds toward Appalachians.

Figure 4 AMSU channel 9 (~80 hPa) radiance perturbation maps at four crossing times during 19-20 January 2003. The crossing time is defined by the orbit crossing the map center. Adjacent orbits are separated by ~100 minutes in time. Two regions, indicated by the boxes, are of special interest in this study. Region 1 (right) is to study GWs propagating off North America, whereas region 2 (left) is used to monitor orographic waves from the Appalachians.

Figure 5 AMSU channel 13 (~5 hPa) radiance perturbation maps at four crossing times during 20-21 January 2003. The crossing time and the two interest regions are defined in the same way as in Figure 4.

Figure 6 Radiance perturbations from N16 AMSU-A channels 9-14 at 6.5Z on 20 January. The peak-to-peak color is indicated in the title.

Figure 7 Vertical cross-section of wave structures as observed from AMSU-A channels 7-14) at ~06Z on January 20. The cross-section is cut through the track indicated by the thick line in Figure 6. The latitude-height plot clearly shows that waves are tilted towards upstream, as expected for the jet streaks generated from instability.

Figure 8 Track and timeline of the wave packet for the first event as seen by channel 13 on 20-21 January 2003. AMSU-A instruments from NOAA-15, 16, 17, and NASA Aqua satellites are used to monitor the wave movement in about every 6 hours from the beginning to the end of this transient event.

Figure 9 Time series of AMSU-A channel 9 radiance variances for regions 1 and 2 in January 2003. The four AMSU-A data have been used to produce the time series and averaged into hourly bins. Data with the number of samples less than 100 per bin are excluded in these plots. The noise floor is $\sim 0.02 \text{ K}^2$ and the solid line is the 3-point running smooth of the data.

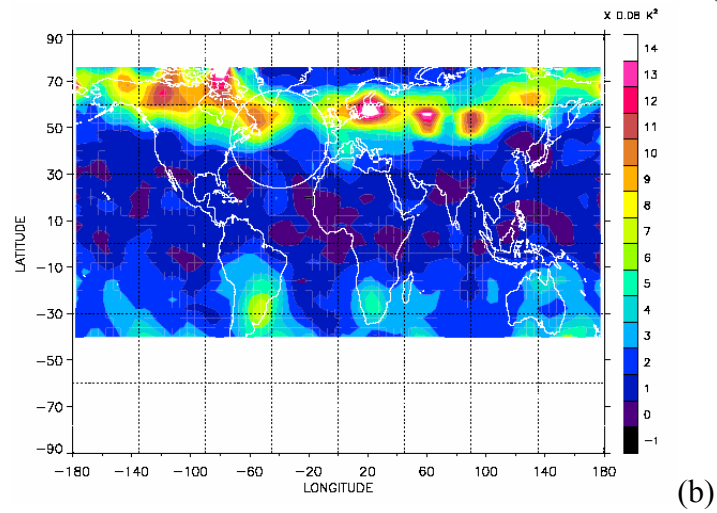
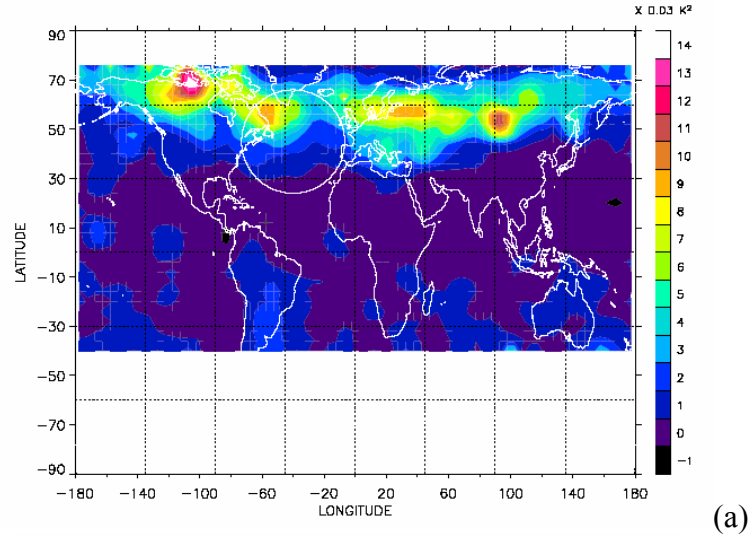
Figure 10 Similar to Figure 9 except for channel 13. The noise floor in this case is $\sim 0.2 \text{ K}^2$.

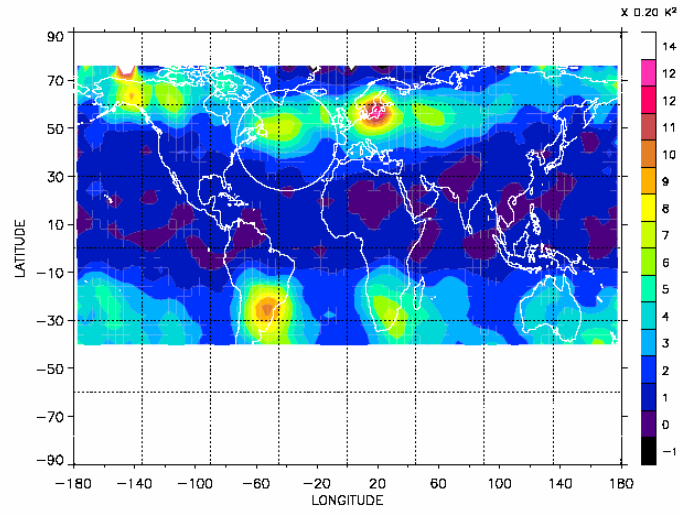
Figure 11 The 80-hPa horizontal divergence (every $3 \times 10^{-5} \text{ s}^{-1}$; blue, positive; red, negative), the 300-hPa geopotential heights (every 20 dam) and horizontal wind speed (shaded) from the MM5 simulations at 18Z on January 19 (starting on January 19, 0Z). The MM5 simulation predicts the two types of GWs seen in AMSU-A channel 9

radiances: one related to jet instability or frontal convection, and the other related to Appalachians.

Figure 12 Vertical profiles of horizontal divergence (every $3 \times 10^{-5} \text{ s}^{-1}$; blue, positive; red, negative) and potential temperature (black, every 8 K). (a) Vertical cross-section (AB) of GWs on January 19 18Z, showing tilted wave structure in the troposphere and lower stratosphere. Horizontal wavelengths of these waves vary between 300-500 km whereas vertical wavelengths are seen between 7-15 km. (b) Vertical cross-section (CD) of GWs over the Appalachians as simulated by MM5. The horizontal and vertical wavelengths in this case are ~ 250 km and ~ 12 km, respectively. The locations of the cross sections are indicated in Figure 11. Dark thick curves denote the dynamic tropopause where potential vorticity equals 1.5 PVU.

Figure 1 GW variance maps from UARS MLS descending orbits for December 1991-January 1992 at 38 km (a), 48 km (b) and 61 km (c). The region over the northwestern Atlantic, highlighted by the circle, is of interest in this study where GWs are frequently generated and propagate into the stratosphere and mesosphere.





(c)

Figure 2 AMSU GW variance maps for December 2002-January 2003 at 80 hPa (~18 km) (a) and 5 hPa (~37 km) (b). Bad measurements are indicated by the white boxes.

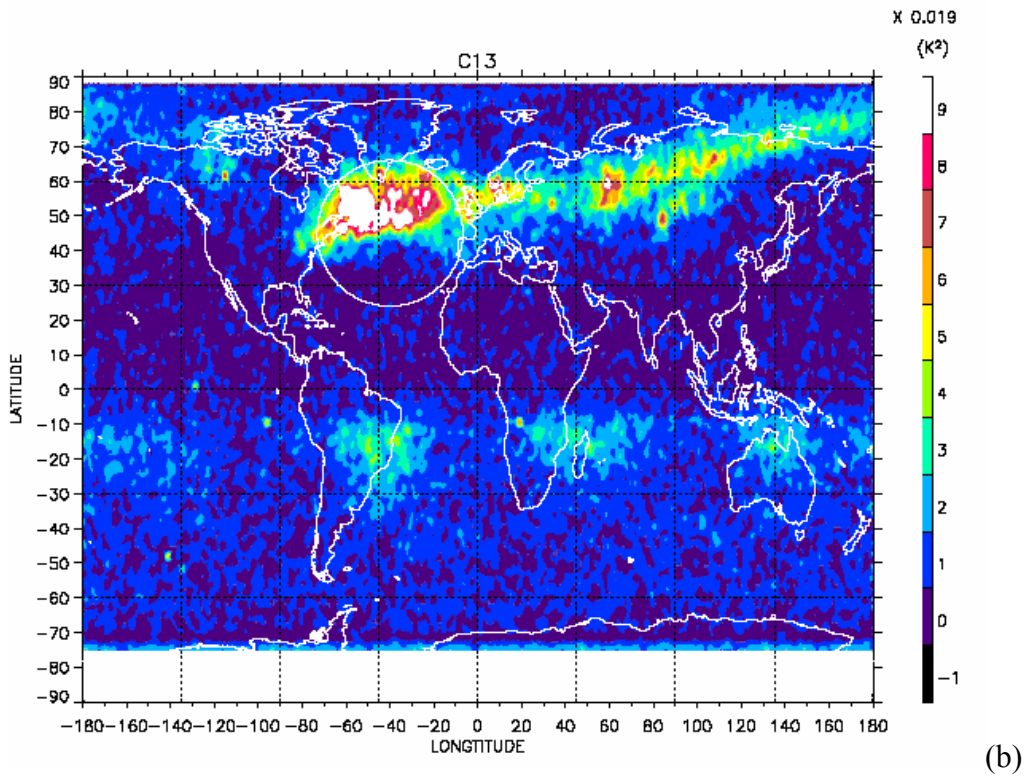
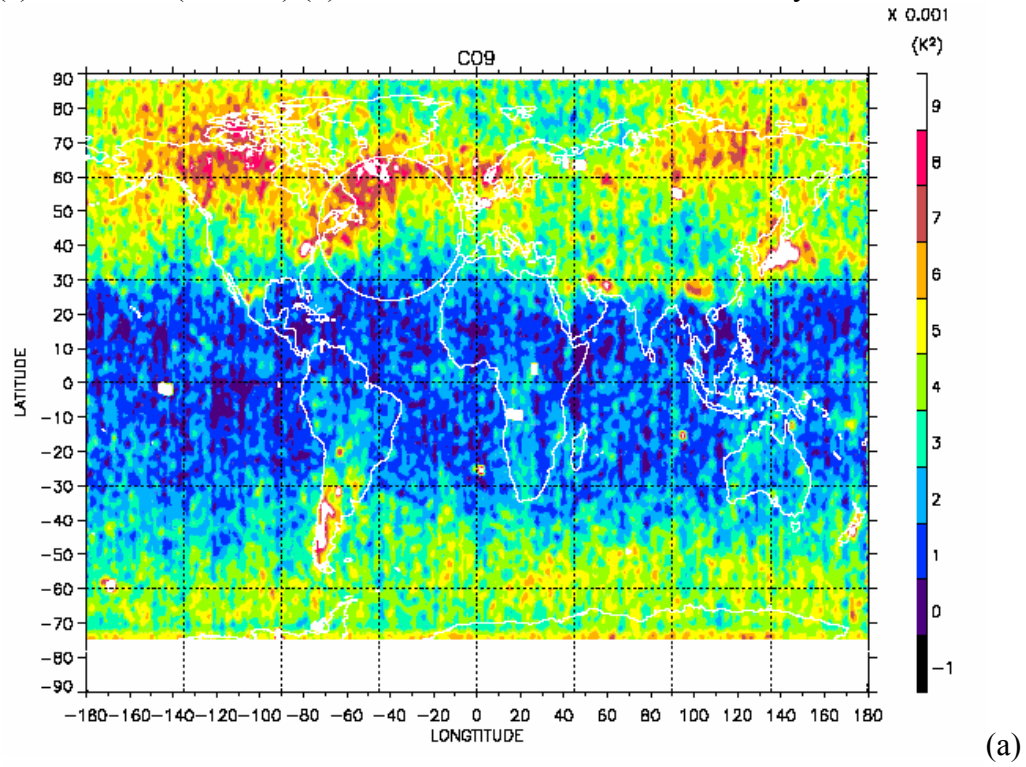


Figure 3 ECWFMF 300-hPa geopotential heights (every 20 dam) and horizontal winds (in vectors, speed greater than 60 m/s shaded) at (a) 00Z on 19 January and (b) 12Z on 20 January 2003. At 12Z on 20 January 2003, the trough moved to the east U.S, creating strong winds toward Appalachians.

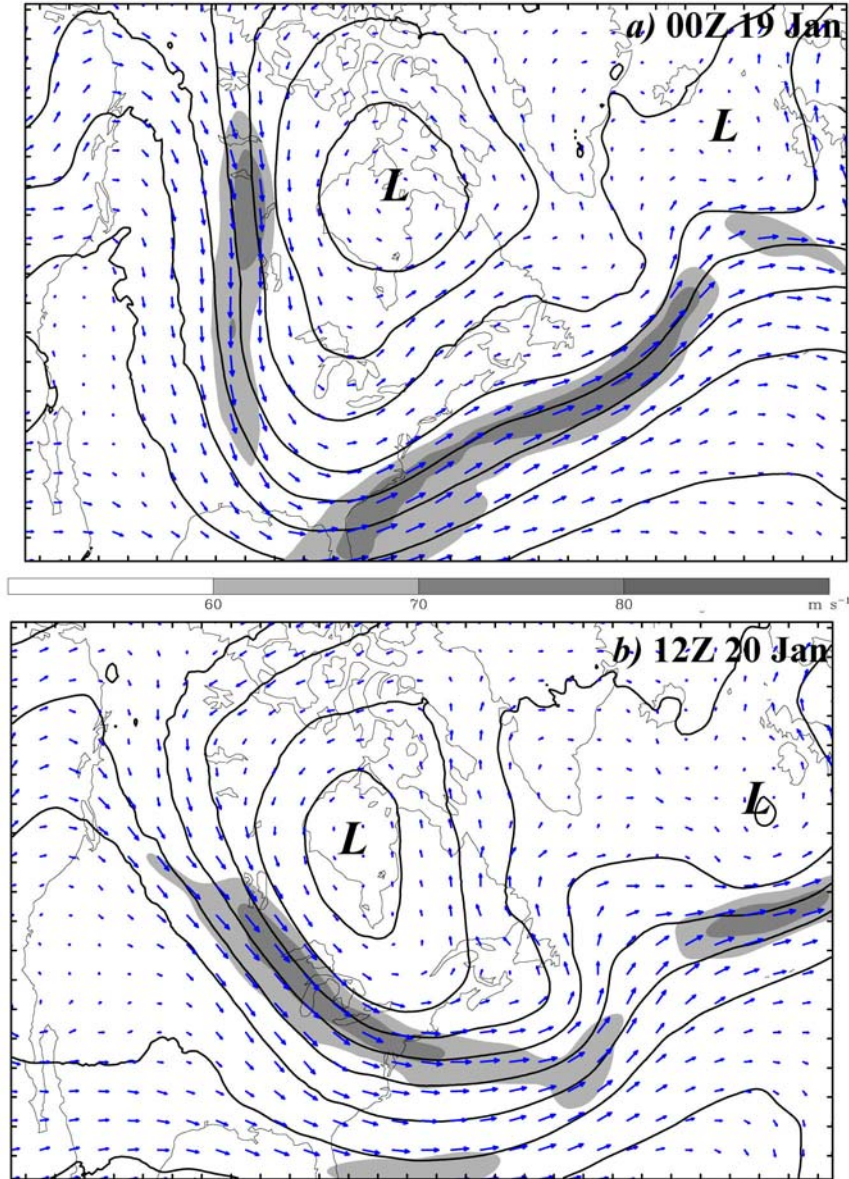


Figure 4 AMSU channel 9 (~80 hPa) radiance perturbation maps at four crossing times during 19-20 January 2003. The crossing time is defined by the orbit crossing the map center. Adjacent orbits are separated by ~100 minutes in time. Two regions, indicated by the boxes, are of special interest in this study. Region 1 (right) is to study GWs propagating off North America, whereas region 2 (left) is used to monitor orographic waves from the Appalachians.

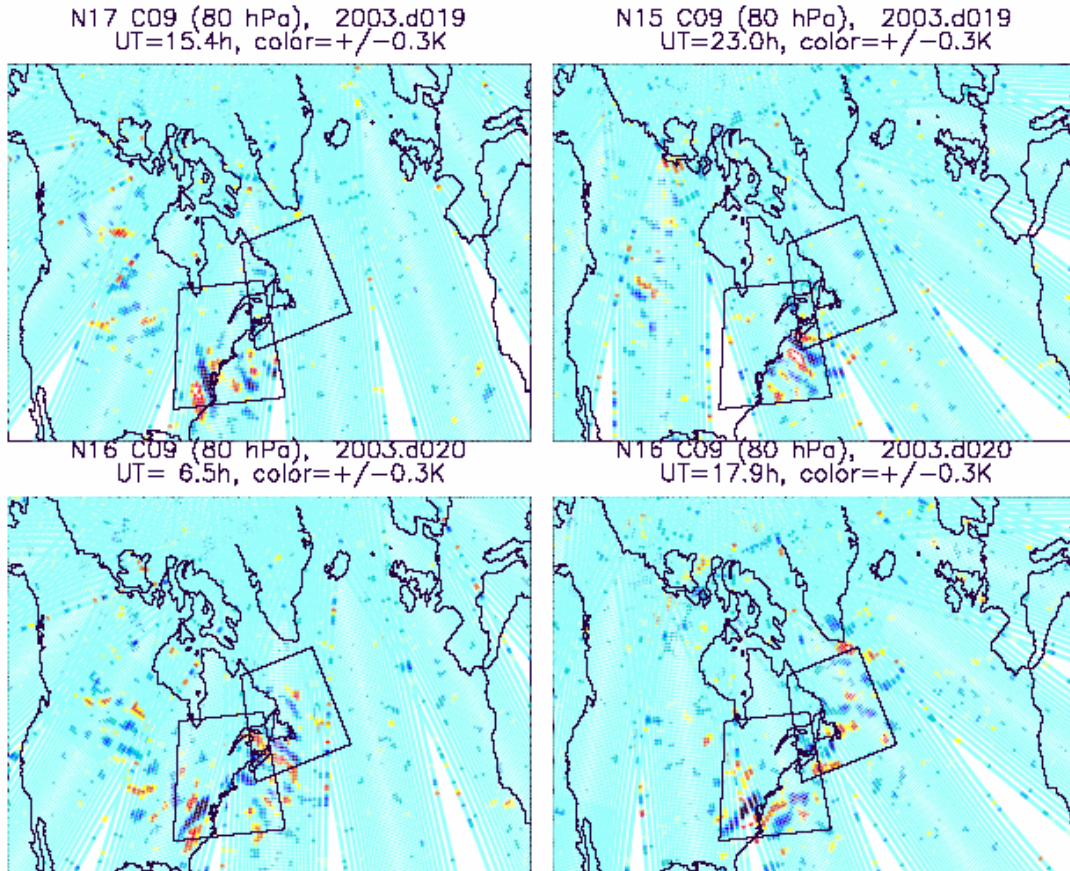


Figure 5 AMSU channel 13 (~5 hPa) radiance perturbation maps at four crossing times during 20-21 January 2003. The crossing time and the two interest regions are defined in the same way as in Figure 4.

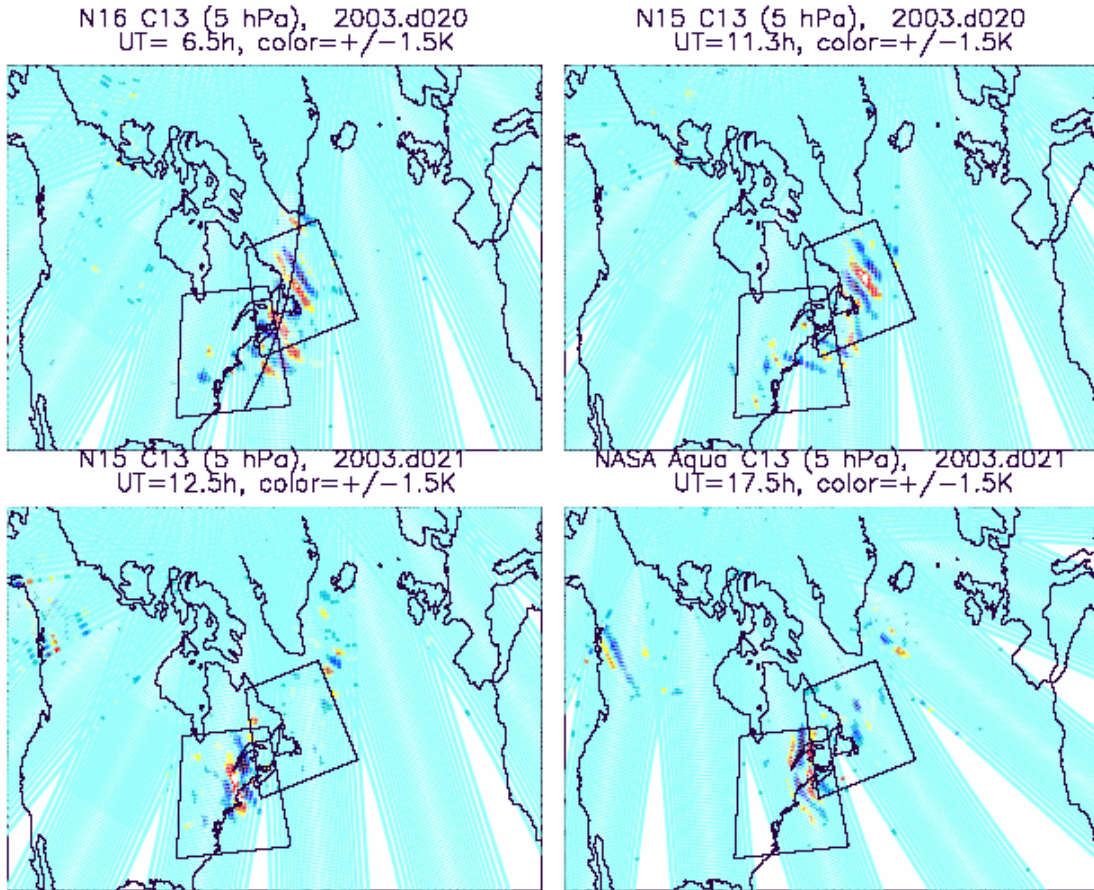


Figure 6 Radiance perturbations from N16 AMSU-A channels 9-14 at 6.5Z on 20 January. The peak-to-peak color is indicated in the title.

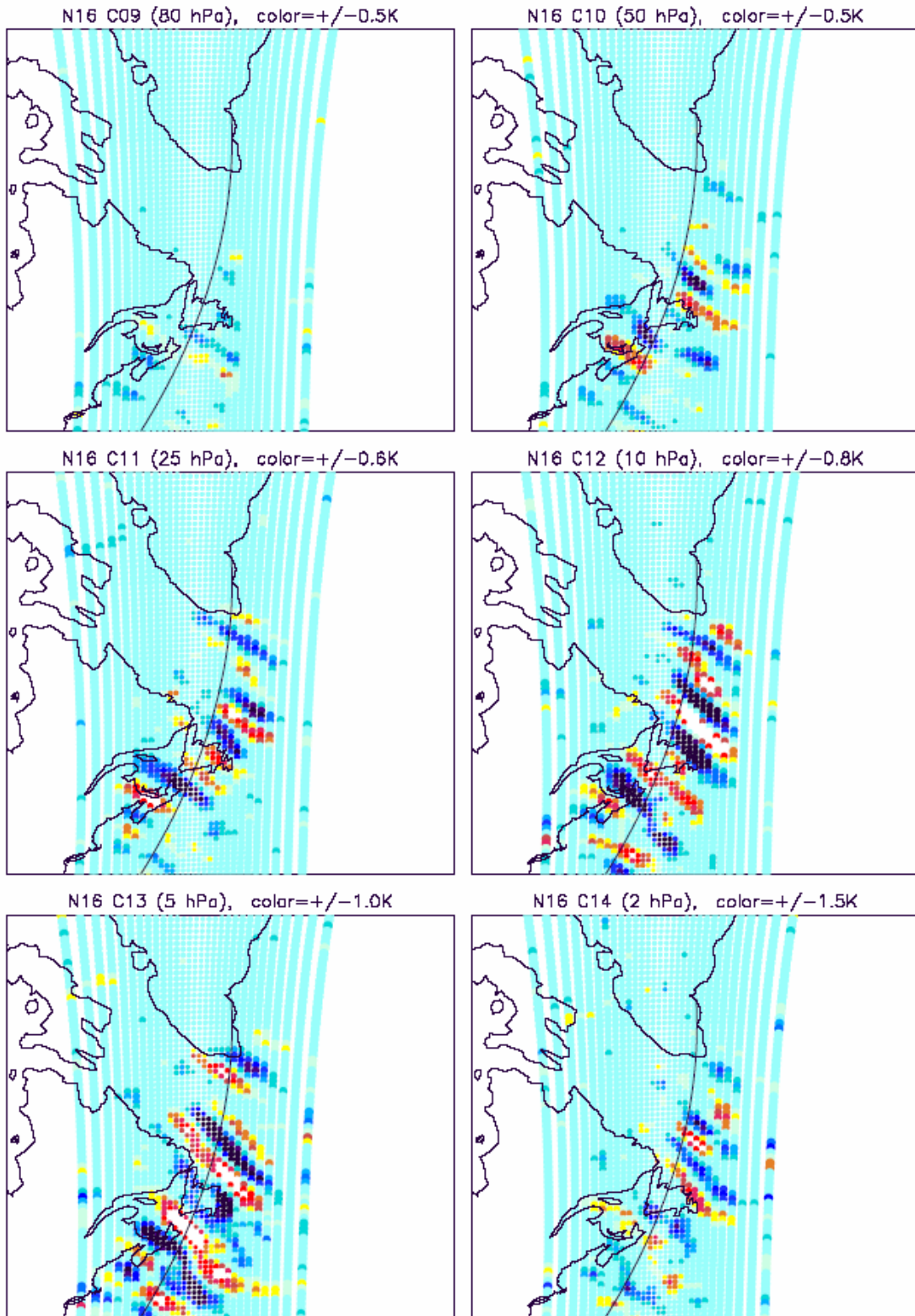


Figure 7 Vertical cross-section of wave structures as observed from AMSU-A channels 7-14 at ~06Z on January 20. The cross-section is cut through the track indicated by the thick line in Figure 6. The latitude-height plot clearly shows that waves are tilted towards upstream, as expected for the jet streaks generated from instability.

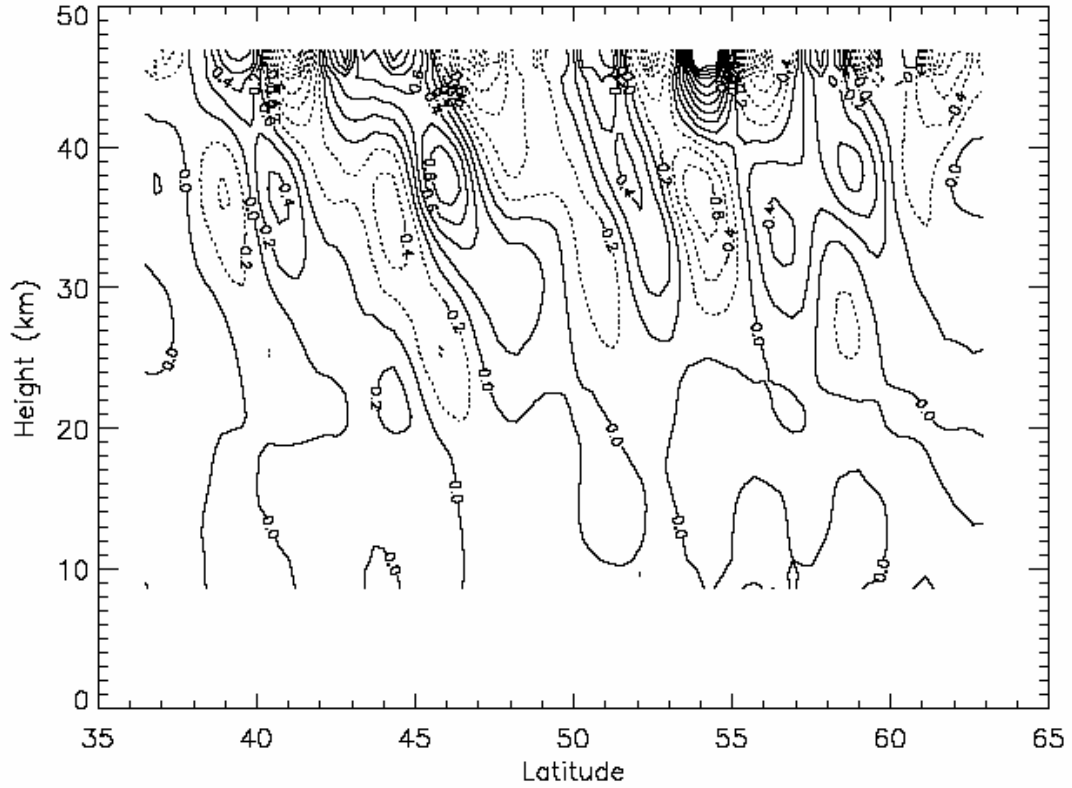


Figure 8 Track and timeline of the wave packet for the first event as seen by channel 13 on 20-21 January 2003. AMSU-A instruments from NOAA-15, 16, 17, and NASA Aqua satellites are used to monitor the wave movement in about every 6 hours from the beginning to the end of this transient event.

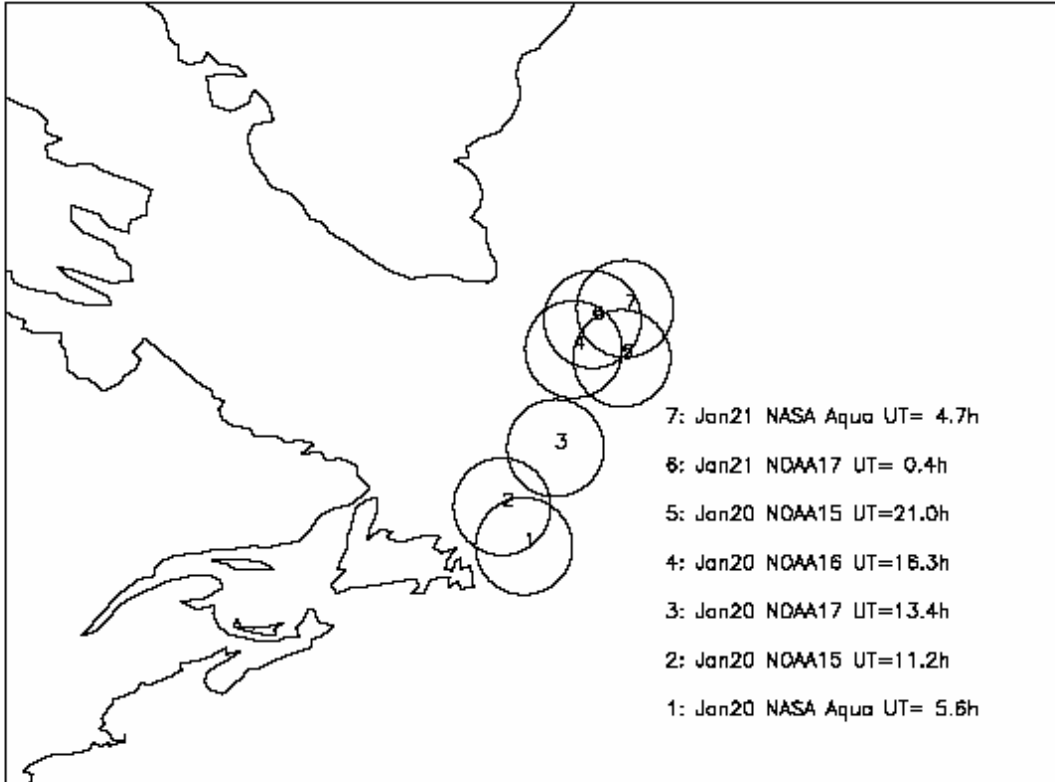


Figure 9 Time series of AMSU-A channel 9 radiance variances for regions 1 and 2 in January 2003. The four AMSU-A data have been used to produce the time series and averaged into hourly bins. Data with the number of samples less than 100 per bin are excluded in these plots. The noise floor is $\sim 0.02 \text{ K}^2$ and the solid line is the 3-point running smooth of the data.

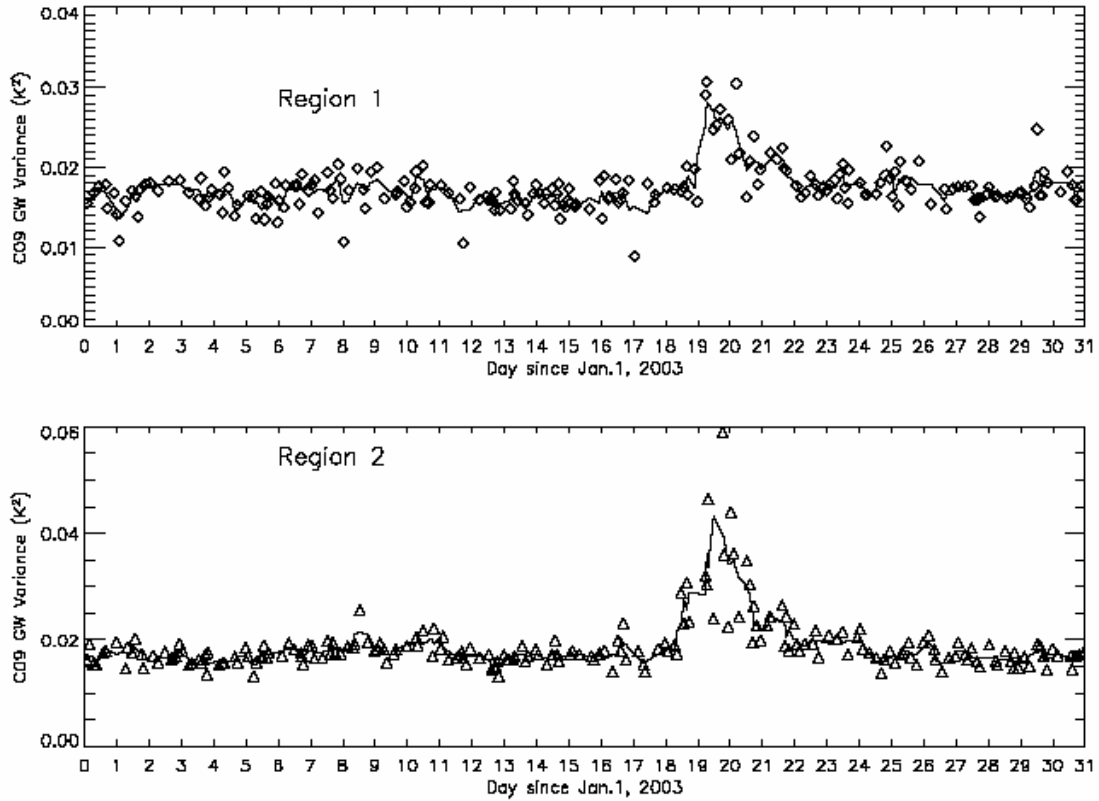


Figure 10 Similar to Figure 9 except for channel 13. The noise floor in this case is $\sim 0.2 K^2$.

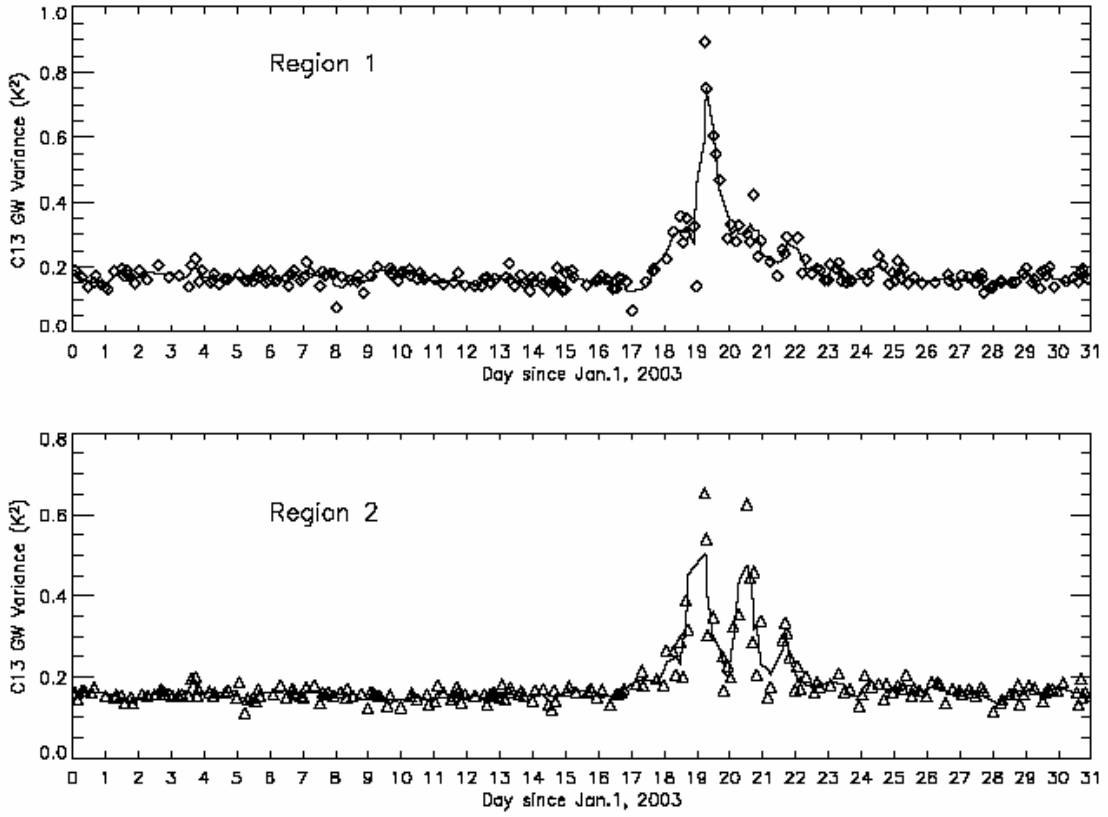


Figure 11 The 80-hPa horizontal divergence (every $3 \times 10^{-5} \text{ s}^{-1}$; blue, positive; red, negative), the 300-hPa geopotential heights (every 20 dam) and horizontal wind speed (shaded) from the MM5 simulations at 18Z on January 19 (starting on January 19, 0Z). The MM5 simulation predicts the two types of GWs seen in AMSU-A channel 9 radiances: one related to jet instability or frontal convection, and the other related to Appalachians.

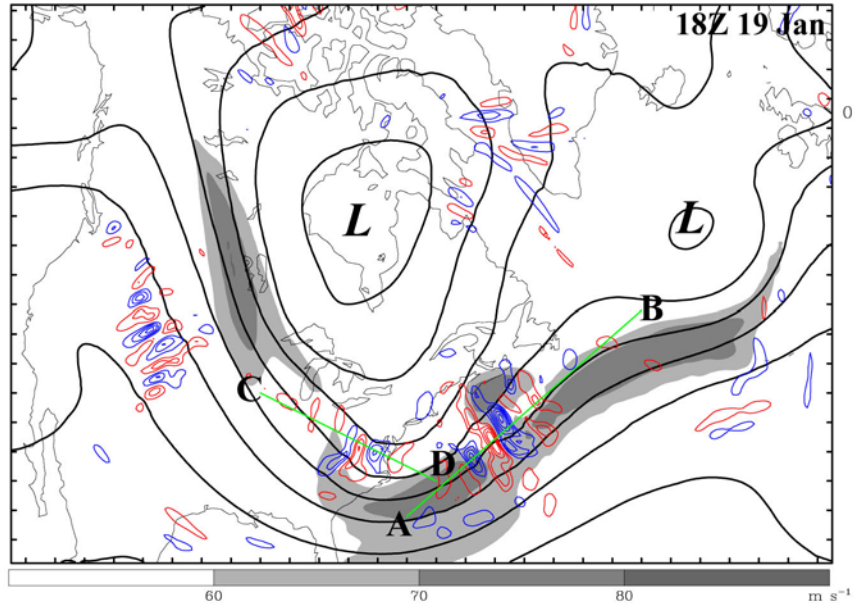


Figure 12 Vertical profiles of horizontal divergence (every $3 \times 10^{-5} \text{ s}^{-1}$; blue, positive; red, negative) and potential temperature (black, every 8 K). (a) Vertical cross-section (AB) of GWs on January 19 18Z, showing tilted wave structure in the troposphere and lower stratosphere. Horizontal wavelengths of these waves vary between 300-500 km whereas vertical wavelengths are seen between 7-15 km. (b) Vertical cross-section (CD) of GWs over the Appalachians as simulated by MM5. The horizontal and vertical wavelengths in this case are $\sim 250 \text{ km}$ and $\sim 12 \text{ km}$, respectively. The locations of the cross sections are indicated in Figure 11. Dark thick curves denote the dynamic tropopause where potential vorticity equals 1.5 PVU.

